

A 28-year-long (1997–2024) hydrographic dataset from the southern Baltic Sea

Daniel Rak¹, Anna Izabela Bulczak¹, Waldemar Walczowski¹, Piotr Wieczorek¹, Małgorzata Merchel¹, Robert Osiński¹, Ilona Goszczko¹, Agnieszka Beszczynska-Moeller¹, Agnieszka Strzelewicz¹, Małgorzata Kitowska¹

¹ Observational Oceanography Laboratory, Institute of Oceanology PAN, Physical Oceanography Department, Sopot, Poland

* Correspondence to: Daniel Rak (rak@iopan.pl)

Abstract. The data set presented here consists of Conductivity–Temperature–Depth (CTD) observations collected during 96 research cruises of R/V *Oceania* across the southern Baltic Sea between 1997 and 2024. The collection comprises towed and vertical station profiles acquired along a repeat transect spanning the Arkona Basin, Bornholm Basin, Słupsk Furrow, and Gdańsk Basin. Acquisition and post-processing procedures include standardized parsing of CNV/TXT files, robust time/position handling, pressure-binning to 1 dbar, median filtering, automated geolocation quality control, and pruning of incomplete profiles. The dataset enables analyses of seasonal to decadal variability in temperature and salinity, inflow propagation, ventilation events, and model validation. Manufacturer specifications for the principal instruments (Guildline 87104, Idronaut OS316/OS316Plus, Sea-Bird SBE49, Sea-Bird SBE19plus) are summarized to inform uncertainty assessment.

1. Introduction

The Southern Baltic Sea, a semi-enclosed marginal sea, forms an important transitional region connecting the North Sea through the Danish Straits. This geographic setting leads to distinct hydrographic conditions characterized by episodic inflows of saline North Sea waters, which strongly influence stratification, deep-water renewal, and regional marine dynamics (Matthäus & Franck, 1992; Mohrholz et al., 2015). The proximity of the Danish Straits exerts a dominant control on hydrography in the region, as episodic inflows of saline North Sea water propagate eastward, shaping stratification and deep-water renewal. Consequently, this region exhibits pronounced vertical stratification patterns driven by inflow events and the progressive downstream modification of water masses with increasing distance from the Danish Straits, coupled with distinct seasonal variability in temperature and salinity (Leppäranta & Myrberg, 2009).

Major Baltic Inflows (MBIs), occur episodically from the North Sea into the Baltic Sea, significantly affecting its hydrography and circulation (Fischer & Matthäus, 1996; Mohrholz et al., 2015). These inflows are classified into two main types: barotropic and baroclinic. Barotropic inflows result primarily from large-scale meteorological forcing, such as prolonged westerly winds, significant changes in atmospheric pressure, and sea level differences between the North Sea and Baltic Sea, causing substantial volumes of saline water to enter the Baltic basins

35 (Burchard et al., 2005; Stigebrandt and Gustafsson, 2003). Baroclinic inflows, on the other hand, are driven by
36 density gradients and stratification differences, often involving internal waves and subsurface transport
37 mechanisms. MBIs transport large volumes of dense, oxygen-rich saline waters into deeper Baltic basins,
38 replenishing oxygen levels in bottom waters and impacting both physical and ecological processes (Mohrholz,
39 2018). The frequency, intensity, and impact of these inflow events are crucial for understanding the long-term
40 environmental status of the Baltic Sea, influencing deep-water renewal and ecosystem dynamics (Reissmann et
41 al., 2009).

42 Comprehensive observational datasets for the Southern Baltic Sea remain relatively scarce, particularly
43 continuous, high-resolution Conductivity-Temperature-Depth (CTD) profiles spanning multiple decades (Feistel
44 et al., 2008). Hydrographic observations in the Baltic Sea are represented in long-standing international data
45 compilations and infrastructures (e.g., ICES data archives, SeaDataNet, EMODnet, Copernicus Marine Service,
46 and global repositories such as the World Ocean Database). However, many historical measurements are spatially
47 heterogeneous or episodic, and a substantial fraction originates from fixed monitoring stations rather than repeated
48 basin-scale sections. In contrast, the IOPAN program provides a rare, long-term, repeatedly sampled transect that
49 consistently links the Arkona Basin, Bornholm Basin, Słupsk Furrow, and Gdańsk Basin, enabling coherent
50 analysis of along-basin hydrographic structure and variability over nearly three decades. While sporadic
51 measurement campaigns and shorter-term datasets exist, long-term, systematic collections are limited, making it
52 challenging to fully understand the variability and long-term trends in the region (Omstedt et al., 2014). This
53 scarcity is especially pronounced within the Polish Exclusive Economic Zone (EEZ), where the availability of
54 openly accessible, high-resolution CTD data is particularly limited. In contrast to the better-monitored central
55 basins of the Baltic Sea—such as the Bornholm and Gotland Basins—data coverage in the Polish EEZ has been
56 historically sparse and fragmented. Regular measurements in this area have often been conducted only a few times
57 per year, and real-time or near-real-time data have not been readily available until the recent deployment of Argo
58 floats (Walczowski et al., 2020). The lack of dense, long-term in situ CTD records hinders detailed analyses of
59 vertical structure, stratification, oxygen dynamics, and long-term hydrographic shifts in this environmentally and
60 economically important sector of the Baltic Sea. Furthermore, this data gap poses significant challenges to
61 numerical modeling, operational oceanography, and marine environmental management.

62 Addressing this critical gap, this article introduces a unique, meticulously curated dataset comprising CTD profiles
63 collected over 28 years (1997–2024) in the Southern Baltic Sea by the Observational Oceanography Laboratory
64 of the Institute of Oceanology Polish Academy of Sciences (IOPAN), Physical Oceanography Department. The
65 data, gathered systematically aboard the research vessel R/V Oceania, provide invaluable insights into the physical
66 oceanographic processes shaping the local environment and their connection to broader climatic phenomena. Some
67 of these data have already been used in previous publications on long-term changes in the southern Baltic Sea,
68 including studies on temperature and salinity (Rak and Wiczorek, 2012), oxygen levels (Rak et al., 2020), the
69 upper ocean mixing and stratification (Bulczak et al., 2024) and the sea energy (Rak et al., 2024), and inflow
70 propagation (Rak, 2016). However, in this work, we make the full dataset publicly available and provide a
71 comprehensive description of its processing and key features.

72 The significance of these measurements lies in their extensive temporal coverage and high spatial resolution, which
73 enable comprehensive analyses of variability across a range of temporal scales—from seasonal to decadal—and
74 spatial scales, from sub-mesoscale to basin-wide. Furthermore, this dataset serves as a vital resource for improving

75 numerical ocean modeling and validation efforts, contributing significantly to our understanding of both local
76 marine dynamics and global climate-related processes (Gröger et al., 2021).

77

78 **2. Study area and campaign design**

79 The repeat hydrographic section follows the axis of the deep basins in the southern Baltic Sea, from the Arkona
80 Basin through the Bornholm Basin and the Słupsk Furrow to the Gdańsk Basin. This section spans approximately
81 280 nautical miles (≈ 519 km), and the measurement time with the towed probe varies from 3 to 5 days, depending
82 on weather conditions.

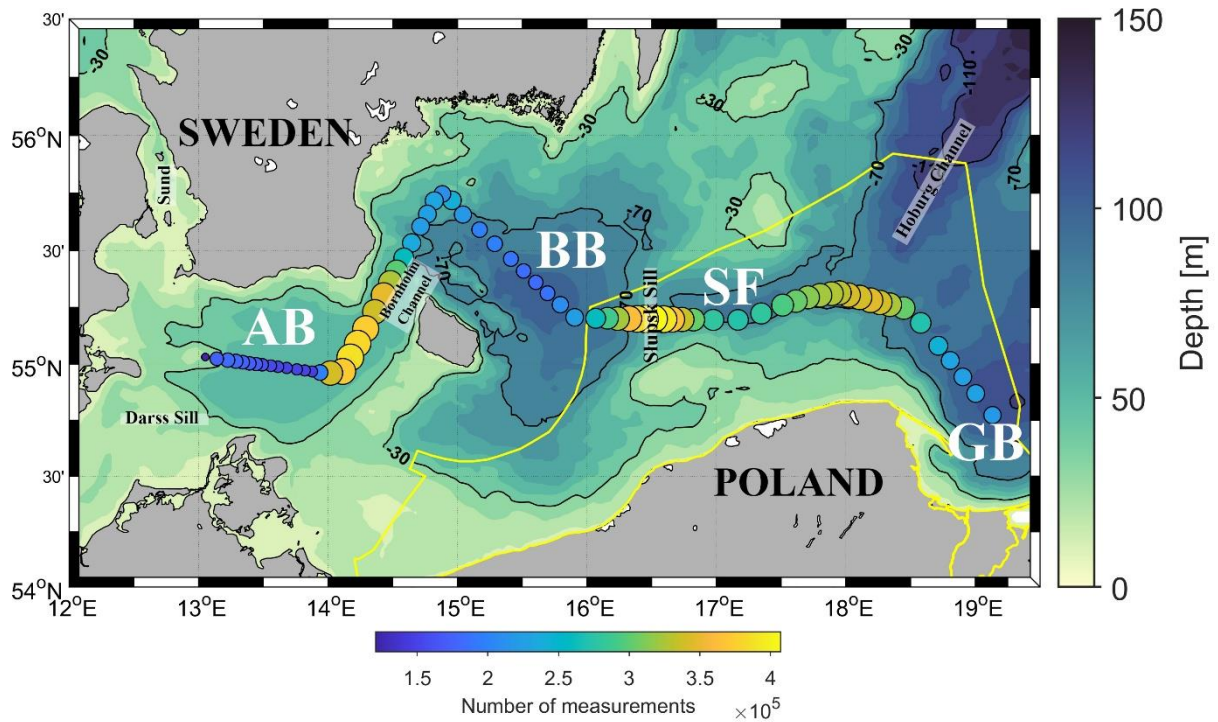
83 Although the monitoring program was originally designed to cover the full transect linking the Arkona Basin,
84 Bornholm Basin, Słupsk Furrow, and Gdańsk Basin, not all cruises achieved complete spatial coverage. Weather
85 conditions, ship-time constraints, and operational limitations occasionally resulted in partial transects or a reduced
86 number of stations. Full-transect coverage was achieved most consistently prior to 2018. In subsequent years,
87 reduced ship time, budget constraints, and operational limitations progressively curtailed the western reach of the
88 section—first to the vicinity of the Bornholm Channel and ultimately to profiles within the Polish Exclusive
89 Economic Zone, which remains the current operational limit. Nevertheless, the Gdańsk Basin and Słupsk Furrow
90 were sampled during the majority of campaigns, ensuring continuity of the key hydrographic time series. Over the
91 28-year period, the dataset therefore represents a quasi-regular repeated section rather than a perfectly uniform
92 annual survey.

93 The transect evolved over time. Since the early 2000s, the core transect from the Bornholm Channel
94 (Bornholmshgat) to the Gdańsk Basin has been performed in a highly repeatable manner. In contrast, the western
95 segment across the Arkona Basin did not follow a single fixed track. Depending on logistics and weather
96 conditions, the route varied between a more northerly pathway oriented toward the Sound and a more southerly
97 pathway closer to the Darss Sill.

98 Over the 28-year period (Figure 1), sampling was designed to capture the pathways and transformation of North
99 Sea inflow waters while maintaining consistent coverage within the Polish sector of the southern Baltic. As a
100 result, data density is highest in the Bornholm Basin, the Słupsk Furrow and Słupsk Sill region, and the Gdańsk
101 Basin, which together form the core observation corridor of the long-term monitoring. To quantify spatial
102 coverage, we classified each cruise by its westernmost extent along the section (based on the westernmost station
103 longitude). Approximately 31% of cruises reached the Arkona Basin, $\sim 62\%$ reached at least the Bornholm
104 Channel, and $\sim 80\%$ reached at least the Bornholm Basin. This variability should be considered when interpreting
105 basin-scale climatologies and the long-term statistics.

106

107



108
 109 **Figure 1: Spatial distribution of CTD profiles collected during R/V Oceania cruises between 1997 and 2024 in the**
 110 **southern Baltic Sea. The yellow line indicates the Polish Exclusive Economic Zone (EEZ). The labels AB, BB, SF and**
 111 **GB denote the Arkona Basin, Bornholm Basin, Slupsk Furrow and Gdańsk Basin, respectively.**

112

113 3. Instruments and measurement modes

114 Hydrographic observations of IOPAN were conducted with several CTD systems (Table 1). Early operations used
 115 a Guildline 87104 and an Idronaut OS316; the OS316 was soon complemented and largely superseded by the Sea-
 116 Bird SBE49 FastCAT. All of these instruments were initially deployed in towed mode (underway profiling). Since
 117 2020, vertical casts (stations) profiling has largely replaced towing, primarily with a Sea-Bird SBE19plus and,
 118 more recently, an Idronaut OS316Plus. No routine discrete water samples for salinity calibration were collected
 119 during the majority of cruises. Salinity quality control relied on manufacturer calibration procedures, pre- and post-
 120 cruise sensor checks, and internal consistency between temperature, conductivity, and density structure. Long-
 121 term stability was additionally assessed through intercomparison between different CTD systems used over the
 122 monitoring period and by verifying the consistency of deep-layer salinity signals during major inflow events.

123

124 **Table 1: Overview of CTD instruments used by IOPAN for hydrographic observations in the southern Baltic Sea**
 125 **between 1997 and 2024. The table lists the main devices and corresponding measurement types conducted during each**
 126 **period.**

Year	CTD system	Measurement type
1997–1999	Guildline 87104	Towed
2000–2002	Idronaut OS316	Towed
2002–2003	Idronaut OS316; Sea-Bird SBE49	Towed

2004–2020	Sea-Bird SBE49; SBE19plus	Towed + vertical casts
2021–2023	Sea-Bird SBE19plus	vertical casts
2023–2024	Idronaut OS316Plus / Sea-Bird SBE19plus	Towed + vertical casts

127

128 During towing, the CTD is mounted in a protective metal frame with an under-slung chain to minimize the risk of
 129 seabed contact. This configuration maintains a stable, near-horizontal probe orientation while providing
 130 mechanical protection (Figure 2). To produce a near-sinusoidal sampling pattern, the probe is cycled repeatedly
 131 between surface and bottom. At a towing speed of ~4 kn, this yields a horizontal resolution of ~200–500 m in
 132 typical water depths of 60–120 m. Towed data are acquired on both the downcast and upcast. Since 2020, vertical
 133 stations with a nominal along-track spacing ~5 nm have replaced towing. Owing to the probe’s mounting and its
 134 orientation relative to the direction of motion, only the downcast is retained for vertical (station) measurements.
 135 The nominal spacing of approximately 5 nautical miles between vertical stations was selected as a compromise
 136 between resolving mesoscale hydrographic structures and maintaining practical survey duration. In the southern
 137 Baltic basins, horizontal density and salinity gradients associated with inflow propagation, halocline tilt, and basin-
 138 scale circulation typically occur on spatial scales of 10–30 km. A 5 nm (~9 km) station interval therefore provides
 139 sufficient resolution to capture these gradients and the structure of the permanent halocline while allowing
 140 completion of the transect within available ship time and weather windows. This spacing has been maintained
 141 consistently over the monitoring period to ensure comparability of sections and long-term variability analyses.

142



143

144 **Figure 2: CTD towed probe system used for the collection of data with Sea-Bird SBE49 (2002-2020)**

145

146 Instrument choice for the towed platform was driven by high sample-rate capability and robust real-time telemetry.
 147 The Sea-Bird SBE19plus has been the primary shipboard profiling CTD on board R/V *Oceania*, whereas the
 148 Idronaut OS316Plus—initially used at stations—has more recently been integrated into a refurbished towed frame.
 149 A further advantage of the OS316Plus is its pass-through interface that allows additional auxiliary sensors (e.g.,

150 dissolved oxygen, turbidity) to be powered and telemetered over a single cable. Manufacturer accuracy
 151 specifications for all instruments used in this program are summarized in Table 2.

152 **Table 2: Manufacturer specifications of conductivity-temperature-depth (CTD) profilers used by the Institute of**
 153 **Oceanology, Polish Academy of Sciences (IOPAN) during long-term hydrographic monitoring in the southern Baltic**
 154 **Sea.**

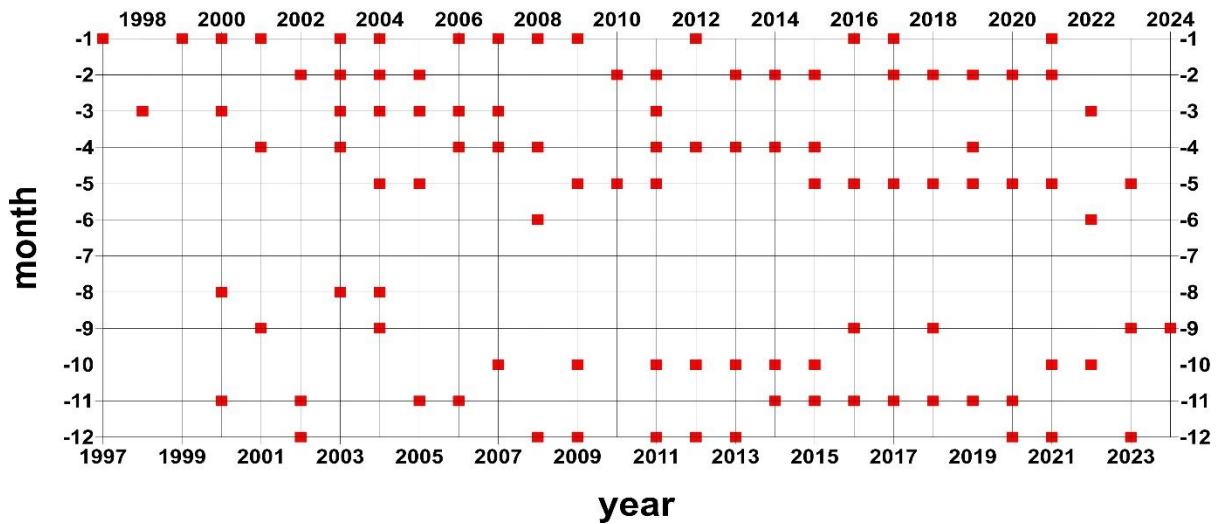
CTD system	Pressure Accuracy	Temperature Accuracy	Conductivity Accuracy	Sampling	Notes
Guildline 87104	(no public spec)	(no public spec)	(no public spec)	(no public spec)	Manufacturer specifications not publicly available.
Idronaut OS316S	±0.05 % FS (0–7000 dbar)	±0.003 °C	±0.0003 S m ⁻¹	4–16 Hz	Full-ocean-depth probe, pump-free, seven-ring quartz conductivity cell.
Idronaut OS316Plus	±0.05 % FS (standard); ±0.01 % FS	±0.002 °C	±0.0003 S m ⁻¹	12–20 Hz (real-time, typically 20 Hz)	Higher precision version, pump-free, 1500 dbar housing.
Sea-Bird SBE49 FastCAT	±0.1 % FS	±0.002 °C	±0.0003 S m ⁻¹	16 Hz	Autonomous CTD for vehicles/ROVs; high sample rate.
Sea-Bird SBE19plus / V2	±0.1 % FS (strain-gauge) / ±0.02 % FS (quartz)	~±0.005 °C	~±0.0005 S m ⁻¹	4–6 Hz	Widely used profiling CTD, V2 offers quartz pressure option.

155

156 4. Dataset and methods

157 Observational data utilized in this study were gathered during research voyages of the Institute of Oceanology of
 158 the Polish Academy of Sciences' vessel, R/V Oceania. These data originated from the Southern Baltic Sea,
 159 spanning the period between 1997 and 2024 (Figure 3). Approximately four surveys were conducted annually,
 160 with the observational program designed to cover the full repeat section linking the Arkona Basin, Bornholm
 161 Basin, Słupsk Furrow, and Gdańsk Basin. In practice, the number of surveys per year varied (typically 2–5)
 162 depending on ship availability, weather, and operational constraints, and not all cruises achieved full spatial
 163 coverage (see Section 2). Owing to the engagement of R/V Oceania in the Arctic research, the period from June
 164 to August is the least represented in the dataset.

165 The temporal sampling is therefore not uniform over the 28-year period. Sampling frequency was the highest in
 166 the early and mid-2000s, when intensive towed surveys provided dense profile coverage, and decreased after 2020
 167 due to the loss of the SBE49 towed system, reduced ship time, and logistical constraints. As a result, the dataset
 168 contains interannual variability in the number of cruises and profiles. This heterogeneity should be considered
 169 when applying statistical methods that assume regular sampling (e.g., long-term linear trend estimation or evenly
 170 spaced climatologies). The dataset is, however, fully suitable for analyses focused on vertical structure, water-
 171 mass variability, stratification, and episodic processes such as inflow and ventilation events, which depend
 172 primarily on profile-scale resolution rather than uniform temporal spacing.

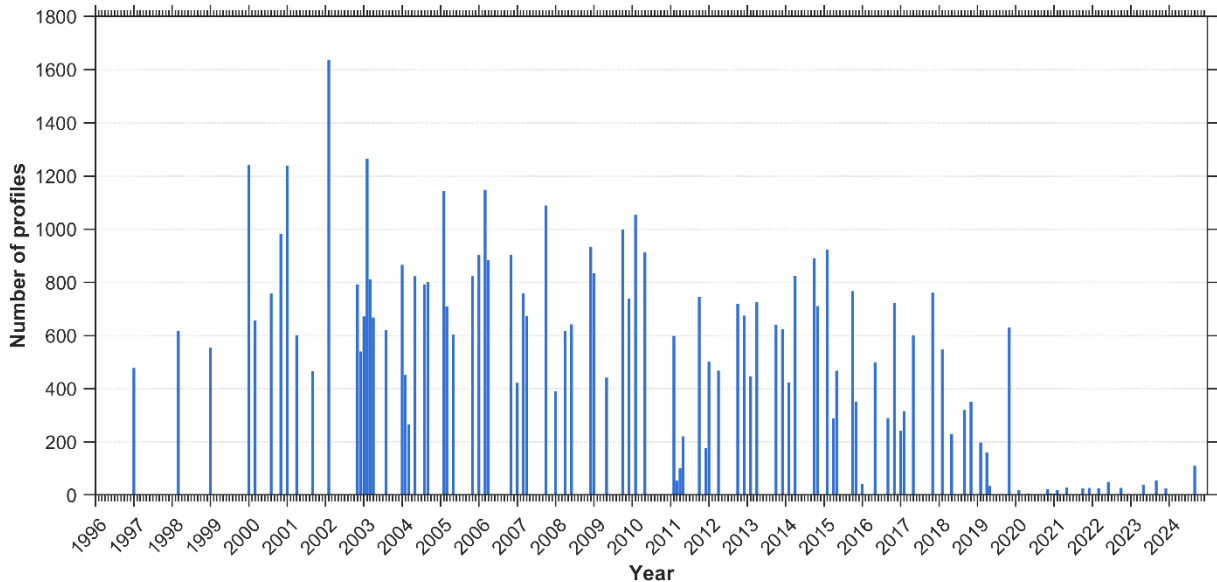


173

174 **Figure 3: Time distribution (1997–2024) of R/V Oceania CTD cruises conducted by the Observational Oceanography**
 175 **Laboratory, Institute of Oceanology PAN.**

176 In total, from 1997 to 2024, 96 hydrographic voyages were conducted, during which 55032 measurement profiles
 177 were recorded (Figure 4). The annual profile counts show strong interannual variability with a clear maximum in
 178 the early–mid 2000s, when intensive towed CTD surveys routinely yielded several hundred to >1,000 profiles per
 179 year. From the late 2000s into the 2010s the effort gradually declined, reflecting reduced sea time and a growing
 180 share of discrete station work. A sharp drop is evident after 2019, consistent with the loss of the SBE49 towed
 181 system in May 2020 and COVID-19 operational constraints; only sparse profiles were collected in 2020–2024.
 182 Overall, the variability primarily reflects instrument availability, cruise logistics, and weather, rather than changes
 183 in processing or quality control.

184



185

186 **Figure 4: Distribution of CTD profiles conducted by IOPAN along the main monitoring transect in the southern Baltic**
 187 **Sea.**

188

189 Towed measurements made with the Guildline 87104, Idronaut OS316, and Sea-Bird SBE49 typically store a
 190 single geographic position and timestamp at the beginning of each profile. Because the probe trails behind the

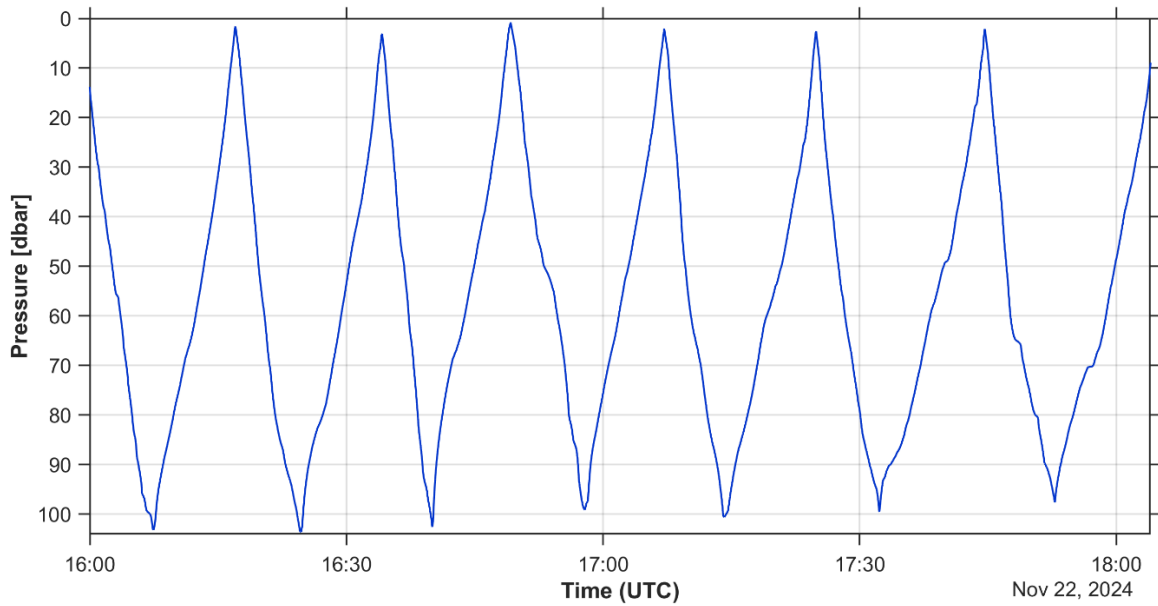
191 vessel on a cable, the actual sampling position deviates from the ship's GPS location. The horizontal offset
192 increases with depth and cable length. A simple geometric upper bound assuming a large cable angle suggests that
193 near-bottom samples could, in extreme cases, be displaced by up to approximately three times the local water
194 depth (e.g., ~300 m at 100 m depth). In practice, however, actual offsets are substantially smaller and remain
195 negligible relative to the mesoscale and basin-scale variability resolved by the section.

196 For vertical (station) profiles, positional uncertainty is much smaller and arises primarily from vessel drift during
197 the cast. In the southern Baltic, station drift is typically modest; when present, it reflects a combination of wind
198 forcing and local currents during the cast, but remains small relative to the nominal station spacing. In systems
199 such as the Idronaut OS316Plus, each sample is associated with a geographic position; however, this corresponds
200 to the ship's GPS location rather than the exact sensor position in the water column. Consequently, a small
201 horizontal offset remains, but it is minor compared to the horizontal scales resolved by the nominal station spacing.
202 As illustrated in Figure 5 for the towed measurements, the descent rate is not uniform: it varies when crossing the
203 pycnocline and with irregular ship motion. Additionally, winch speed is routinely reduced near the surface and
204 close to the seabed for safety reasons, further modulating sampling speed.

205
206 From 1997 to 2020, towed operations were routine. On 20 May 2020 the towed system carrying the Sea-Bird
207 SBE49 was lost; since then, measurements have been conducted predominantly as vertical station casts, with
208 limited towing resumed in 2023–2024 using a refurbished frame. In the post-2020 period, towing is applied
209 selectively due to weather constraints and reduced ship time (typically ~7-day cruises vs ~14 days in earlier
210 intensive periods, e.g., around 2003), and is therefore combined with a reduced set of station casts.

211 The number of cruises decreased after 2020, leading to a temporal discontinuity in sampling frequency.
212 Accordingly, analyses that require regular annual sampling, such as precise decadal trend estimation, should be
213 interpreted with caution. However, the dataset remains fully suitable for studies of vertical structure, stratification,
214 water-mass variability, and episodic events (e.g., inflows and ventilation), which depend primarily on profile-scale
215 resolution. Complementary observations from Argo floats and global data archives provide additional regional
216 context during periods of reduced ship-based sampling, although they generally lack the spatial focus and
217 repeatability of the IOPAN section.

218
219
220



221
 222 **Figure 5: Example of a typical continuous CTD probe trajectory in the water column during towed measurements.**

223

224 **4.1 Instrument calibration and uncertainty budget**

225 All Sea-Bird sensors used in this dataset (SBE 49 FastCAT, Sea-Bird SBE19plus / V2) were regularly returned to
 226 Sea-Bird GmbH (Kempton, Germany) for servicing and post-cruise calibration, typically every 1–3 years,
 227 depending on instrument usage and cruise schedules. Service reports document routine post-cruise calibration of
 228 temperature and conductivity sensors, calibration of pressure sensors, firmware updates and full system checks for
 229 the SBE 49 FastCAT and associated pump and conductivity modules.

230 For the most frequently used CTD on the towed system (Sea-Bird SBE 49 FastCAT), the latest post-cruise
 231 calibration performed in March 2018 yielded extremely small residuals relative to laboratory standards.
 232 Temperature calibration over the range 1–32.5 °C showed residuals within ± 0.0001 °C, i.e. more than an order of
 233 magnitude smaller than the nominal manufacturer accuracy.

234 Conductivity calibration residuals were on the order of 10^{-4} S m⁻¹ across the full range of bath salinities, i.e.
 235 negligible compared to the nominal conductivity accuracy.

236 Pressure calibration for the 870-psia (≈ 600 dbar) pressure sensor showed residuals within ± 0.01 % of full scale,
 237 effectively at the limit of the calibration procedure.

238 Based on manufacturer specifications and these post-cruise calibration results, we adopt conservative instrumental
 239 uncertainties of ± 0.005 °C for temperature, ± 0.01 in practical salinity and ± 0.5 dbar for pressure for individual 1-
 240 dbar binned measurements from Sea-Bird CTDs. These values are larger than the formal calibration residuals, but
 241 they account for potential long-term sensor drift between service intervals and any residual biases introduced by
 242 data processing (vertical binning, median filtering) and deployment configuration (e.g. slight lags due to pump
 243 response and flow through the conductivity cell). For other CTD models used earlier in the time series (Guildline
 244 87104, Idronaut OS316), we adopt comparable or slightly larger uncertainties consistent with manufacturer
 245 specifications and our internal cross-comparisons (Table 3). The Idronaut OS316Plus was factory-calibrated at
 246 Idronaut (24 Nov 2025). Although the dataset analysed here ends in 2024, we report the most recent factory
 247 calibration to document instrument performance and to motivate the conservative uncertainties adopted for the

248 processed products. Calibration residuals were within ± 0.0011 °C for temperature and ± 0.0039 mS/cm for
 249 conductivity. For consistency with the long-term record and to account for drift between service intervals and
 250 processing effects, we adopt conservative uncertainties of ± 0.005 °C, ± 0.01 PSU, and ± 1 dbar for 1-dbar binned
 251 products.

252

253 **Table 3: Overview of the main CTD instruments used in the dataset and the conservative instrumental uncertainties**
 254 **adopted for temperature, practical salinity (PSS-78; reported here in PSU) and pressure.**

Period	Main CTD model	Calibration interval	Temperature uncertainty (°C)	Salinity uncertainty (PSU)	Pressure uncertainty (dbar)
1997–1999	Guildline 87104	No data	No data	No data	No data
2000–2003	Idronaut OS316	every 3 years	± 0.01	± 0.02	± 1
2004–2020	SBE 49 / SBE19plus	every 1–2 years	± 0.005	± 0.01	± 0.5
2023–2024	Idronaut OS316Plus	every 2 years	± 0.005	± 0.01	± 1

255

256 In addition to instrumental uncertainties, there is a finite spatial representativeness error associated with towed
 257 sections. During towing, the CTD is pulled astern and may therefore be horizontally displaced from the ship’s GPS
 258 position. Simple geometric considerations show that an extreme upper bound of three times the local depth would
 259 require the tow cable to be almost horizontal, which is unrealistic for our operating conditions (towing speeds of
 260 ≈ 4 kn and depths of 60–100 m). In practice, observed cable angles correspond to horizontal offsets of the order
 261 of 0.3–0.8 times the local depth; for the error budget we therefore adopt the local depth as a conservative upper
 262 limit on horizontal position uncertainty (≈ 100 m at 100 m depth), while typical offsets are likely closer to 0.5
 263 times the depth. We therefore recommend that the dataset be used primarily for basin-scale and mesoscale
 264 analyses, rather than for resolving fine-scale ($< O(100$ m)) frontal structures, where unresolved horizontal offsets
 265 may become non-negligible.

266 5. Quality check and postprocessing of CTD data

267 The quality control (QC) and postprocessing procedures applied to the CTD data collected by IOPAN are essential
 268 for ensuring the scientific value, internal consistency, and long-term usability of the dataset. Raw data were
 269 recorded using several CTD systems operated over the multi-decade period and were calibrated according to
 270 manufacturer recommendations. Thermal-lag (temperature–conductivity misalignment) effects were addressed
 271 during standard instrument preprocessing prior to salinity computation. Subsequent pressure sorting, 1-dbar
 272 binning, and median filtering further reduce residual high-frequency noise while preserving mesoscale gradients.
 273 Postprocessing starts with an automated MATLAB routine that imports CNV/TXT files and parses station
 274 metadata (date/time and geographic coordinates). Raw samples are first screened for common acquisition artefacts:

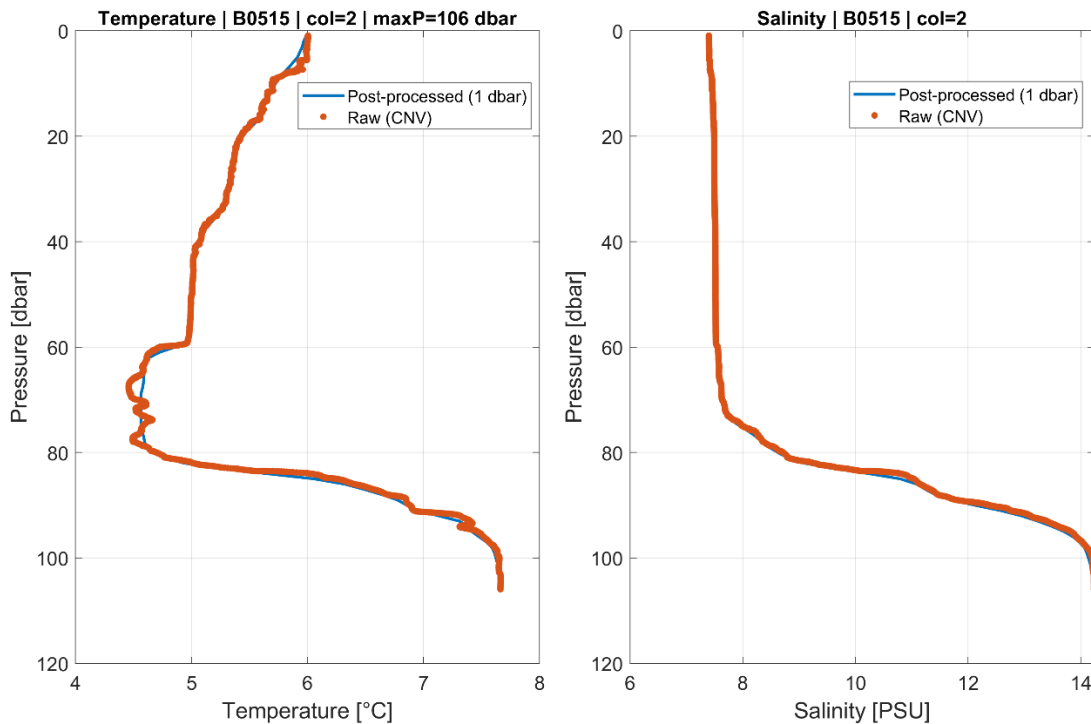
275 records with negative pressure ($p < 0$ dbar) are removed, and instrument fill values (e.g., -9.990×10^{-29}) are
276 converted to NaN. Each cast is then sorted by pressure, repeated pressure levels are consolidated by averaging,
277 and the profile is standardized onto a uniform vertical axis (0–199 dbar, $\Delta p = 1$ dbar) using local averaging within
278 a ± 1 dbar window around each target level. Temperature and salinity are denoised using a running median filter
279 (movmedian, window size typically 20 samples, omitting NaNs). Profiles with missing or invalid metadata are
280 excluded by masking casts where longitude/latitude/time are equal to 0 or NaN. For the gridded processing stream,
281 navigation is additionally quality-checked using broad domain limits (lon 13–22°E, lat 54.2–58°N) and a despiking
282 rule that flags positions deviating by more than 0.1° from a 5-point running median; flagged lon/lat/time values
283 are propagated as a common mask across variables.

284 Hydrographic variables are further checked for physically implausible values and unstable segments. Salinity is
285 constrained to a plausible range (7.2–21), with values outside this range set to NaN. The adopted salinity range is
286 based on the long-term hydrographic characteristics of the southern Baltic Sea. These limits are consistent with
287 regional climatological conditions and historical monitoring data. The vast majority of observations throughout
288 the 28-year record fall within this interval. Values outside the adopted range therefore represent clear outliers
289 attributable to measurement artefacts or processing errors rather than physically plausible hydrographic conditions.
290 A single conservative salinity range was applied uniformly across all basins as part of the automated QC pipeline,
291 to avoid spatially dependent filtering and ensure consistent treatment of all profiles.

292 A static-stability check based on TEOS-10 density was applied. Adjacent levels implying any density inversion
293 ($\Delta \rho < 0 \text{ kg m}^{-3}$) were flagged as unstable, and the corresponding salinity values were set to NaN. Profiles are
294 truncated below the first occurrence of ≥ 5 consecutive NaNs in salinity, and casts exhibiting an abrupt salinity
295 decrease larger than 0.01 between adjacent levels are terminated from that depth downward. For the gridded
296 product, an additional optional vertical smoothing step is applied using a moving mean (smoothdata, window 10)
297 to reduce residual small-scale noise while retaining vertical gradients.

298 After automated QC and postprocessing, profiles are aggregated into structured arrays, enabling downstream
299 climatological and statistical analyses. The processed data are routinely visualized to identify potential outliers
300 and systematic artefacts, and a manual review complements the automated steps, particularly for casts affected by
301 strong ship motion or transient sensor behaviour. To illustrate the effect of our pipeline, Figure 6 contrasts a raw
302 cast with its post-processed counterpart for cruise B0515. This cast was selected as a stress-test case with
303 pronounced motion/sensor transients near the halocline. Residual small-scale noise visible in the raw data is only
304 lightly attenuated by design: our post-processing is intentionally conservative to preserve mesoscale gradients and
305 avoid over-smoothing that could bias stratification metrics.

306



307

308 **Figure 6: Example of a raw CTD profile and the same profile after post-processing. Raw CNV samples (dots) and the**
 309 **1-dbar product (solid line) are shown for temperature (°C) and salinity (PSU); pressure increases downward (dbar).**

310

311

312 6. Data structure and export

313 The dataset is delivered in two interoperable formats. First, as a single MATLAB container in which each cruise
 314 is stored as a separate field of the top-level struct IOPAN. Cruise fields follow the BMMYY convention (B –
 315 Baltic; MM – month; YY – year; e.g., B0523 for May 2023) and contain gridded, column-oriented hydrographic
 316 profile matrices together with a shared vertical coordinate. Second, the same cruise-wise products are exported as
 317 a collection of per-cruise NetCDF files (IOPAN_BMMYY.nc) compliant with the CF-1.8 conventions and the
 318 discrete sampling geometry (DSG) profile representation, with depth × profile hydrographic variables and profile-
 319 wise (1-D) geolocation and time coordinates.

320

321 MATLAB (IOPAN_Baltic.mat)

322 For each cruise:

- 323 • Pressure, Temperature, Salinity: size $N \times M$, where rows are 1-dbar levels and columns are individual profiles.
- 324 • Pressure_string: size $N \times 1$, the common vertical grid (e.g., 0:1:199 dbar).
- 325 • Time (MATLAB datenum), Longitude, Latitude: stored as size $N \times M$ for convenience and co-registration with
 326 the hydrographic matrices; within each profile (column) these values are constant with depth (i.e., they represent
 327 station-level metadata repeated along the vertical). Timestamps represent MATLAB serial days (fractional part =
 328 time of day) and should be interpreted as UTC unless stated otherwise.

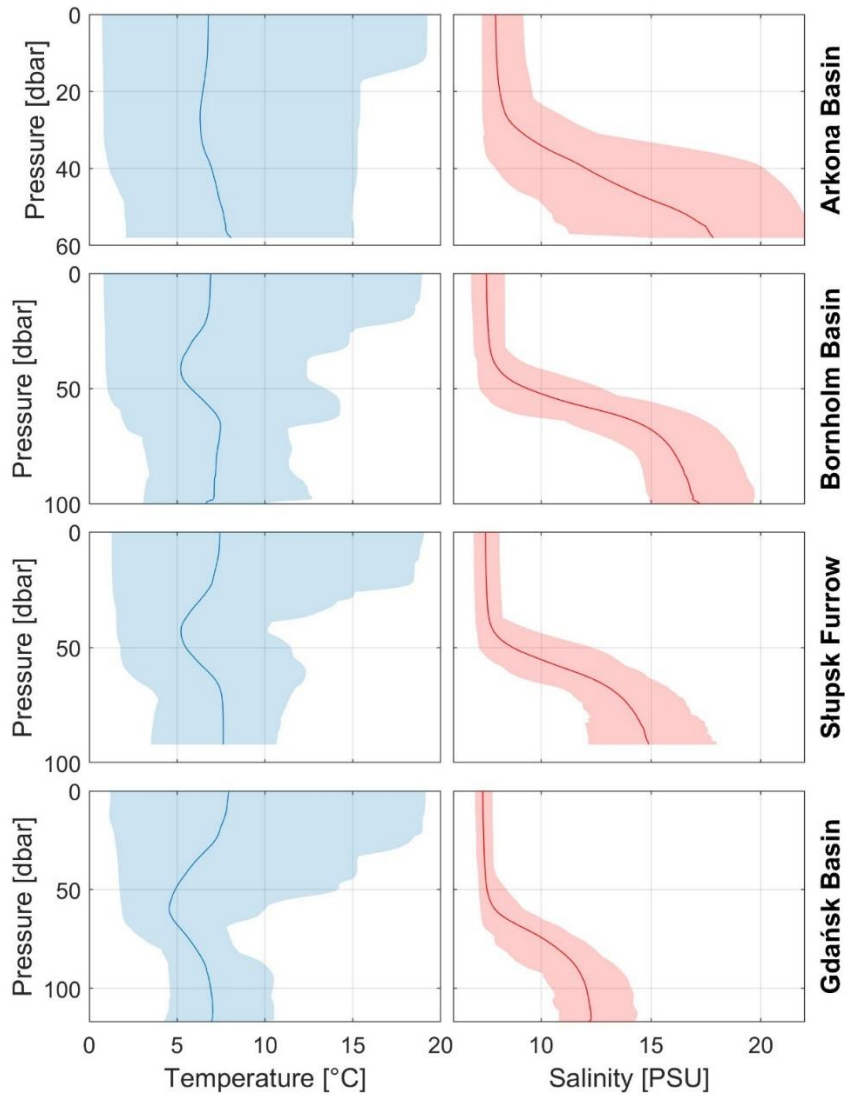
329

330 NetCDF (IOPAN_BMMYY.nc)

331 The NetCDF files use a compact CF-DSG layout in which:
332 • Hydrographic variables are stored on a common pressure grid (dbar) as 2-D arrays with dimensions (pressure,
333 profile), with 1-D coordinates lon(profile), lat(profile), and time(profile).
334 • Coordinates lon(profile) and lat(profile) are stored as 1-D profile-wise variables.
335 • Time is provided as a 1-D CF-compliant coordinate time(profile) (e.g., seconds since 1970-01-01 00:00:00 UTC,
336 calendar = gregorian).
337 During export, the station-level time and position are obtained from the MATLAB N×M matrices by extracting a
338 representative value per profile (e.g., the first finite value in each column).
339 A metadata block accompanies the cruise fields and documents units, creation timestamp, ownership and contact
340 point. Missing or filtered values are encoded as NaN in MATLAB and as _FillValue in NetCDF; pruning during
341 processing removes empty profiles (all-NaN columns) and ensures consistent dimensions within each cruise. The
342 processing and export workflow is implemented in the MATLAB scripts build_IOPAN_from_CNV_TXT.m and
343 write_IOPAN_to_netcdf.m (Zenodo, <https://doi.org/10.5281/zenodo.17814769>).

344 **7. Basin-scale hydrographic structure and variability**

345 Basin-scale vertical structure along the repeat transect is summarized in Figure 7. In all four basins, the upper ~40–
346 60 dbar are dominated by seasonally varying, relatively fresh surface waters, as reflected in the broad temperature
347 envelope and modest salinity range. Below the seasonal thermocline, temperature variability is much reduced,
348 while salinity exhibits a pronounced step-like increase across the permanent halocline. Below ~50 dbar, salinity
349 variability increases markedly compared with the upper layer. This depth range corresponds to the permanent
350 halocline that separates the seasonally mixed brackish surface waters from deeper, more saline North Sea–derived
351 water masses. Variability at depth is therefore governed by episodic inflow events, lateral spreading of saline
352 intrusions, and isopycnal mixing, while the upper layer is more frequently homogenized by wind-driven and
353 seasonal mixing processes. The mean halocline depth and deep salinity systematically change along the section:
354 in the shallow Arkona Basin stratification is generally confined to the upper water column; however, during inflow
355 periods this basin often contains some of the highest salinities observed along the section and can exhibit a
356 pronounced halocline extending from ~30 dbar to the bottom. Farther east, the Bornholm Basin and Słupsk Furrow
357 display strong, well-defined haloclines overlying more saline deep waters. Toward the Gdańsk Basin, deep
358 salinities decrease and the halocline shoals slightly, consistent with progressive dilution and mixing of North Sea
359 inflow waters along their downstream pathway. The shaded ranges highlight that, despite substantial interannual
360 and event-scale variability, the basic vertical structure and along-transect contrasts between basins are robust
361 features of the 28-year record.
362



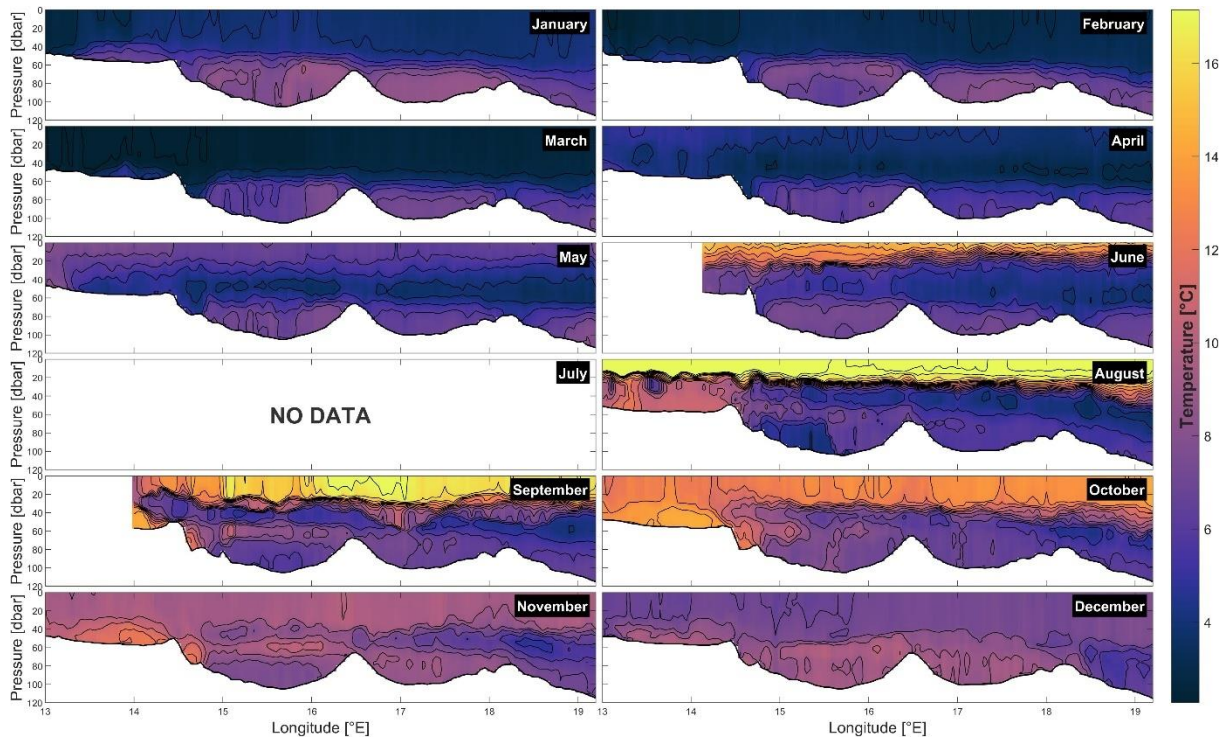
363

364 **Figure 7: Basin-mean vertical profiles of temperature and salinity in the Arkona Basin, Bornholm Basin, Ślupsk Furrow**
 365 **and Gdańsk Basin derived from all CTD casts collected along the repeat section between 1997 and 2024. Solid lines**
 366 **indicate the multi-year mean and shaded envelopes the full range (min-max) across all cruises.**

367

368 Monthly mean temperature sections (January–December) along the repeat Baltic transect are shown in Figure 8.
 369 The 12-panel climatology highlights the pronounced seasonal cycle of the upper water column, with winter cooling
 370 and a deep, relatively homogeneous mixed layer followed by spring onset of stratification, summer surface
 371 warming and development of a shallow thermocline, and an autumnal erosion of stratification. A persistent
 372 dichothermal (cold intermediate) layer is visible from approximately April through November, reflecting winter-
 373 cooled water retained below the seasonal thermocline while the surface layer warms. Along-transect differences
 374 reflect the changing basin geometry and hydrographic regime from the Arkona Basin through the Bornholm Basin
 375 and Ślupsk Furrow toward the Gdańsk Basin, and the month-to-month variability in deeper layers suggests that
 376 advection plays a key role in shaping the subsurface temperature field along the monitoring section.

377



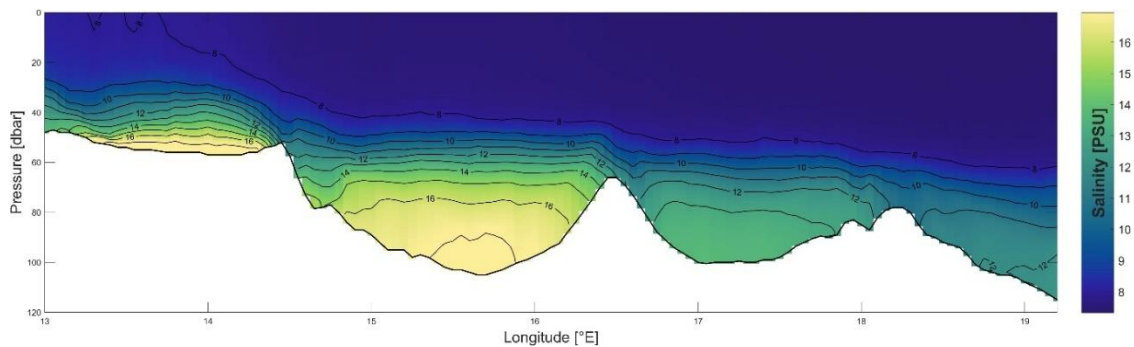
378

379 **Figure 8: Monthly mean temperature sections (January–December) along the Baltic transect as a function of longitude**
 380 **(°E) and pressure (dbar).**

381

382 In contrast to temperature, salinity does not exhibit a pronounced seasonal cycle. Surface salinity variability is
 383 mainly influenced by episodic freshwater input, vertical mixing, and horizontal advection, while deeper salinity
 384 variability reflects irregular advective and mixing processes rather than seasonally phase-locked forcing. Because
 385 salinity variability is dominated by these irregular and spatially structured processes rather than a repeatable annual
 386 cycle, its large-scale characteristics are more clearly represented by the multi-year mean section. Figure 9 shows
 387 the multi-year mean salinity section along the repeat southern Baltic transect. The upper ~40–60 dbar is dominated
 388 by relatively fresh surface waters, while a distinct step-like increase in salinity below marks the permanent
 389 halocline; this halocline is most pronounced over the Bornholm Basin and Słupsk Furrow, which also host the
 390 highest salinities in deeper layers. Farther east toward the Gdańsk Basin, deep salinity decreases and the halocline
 391 structure changes along the section, reflecting the along-transect hydrographic contrasts and downstream
 392 modification of more saline waters.

393

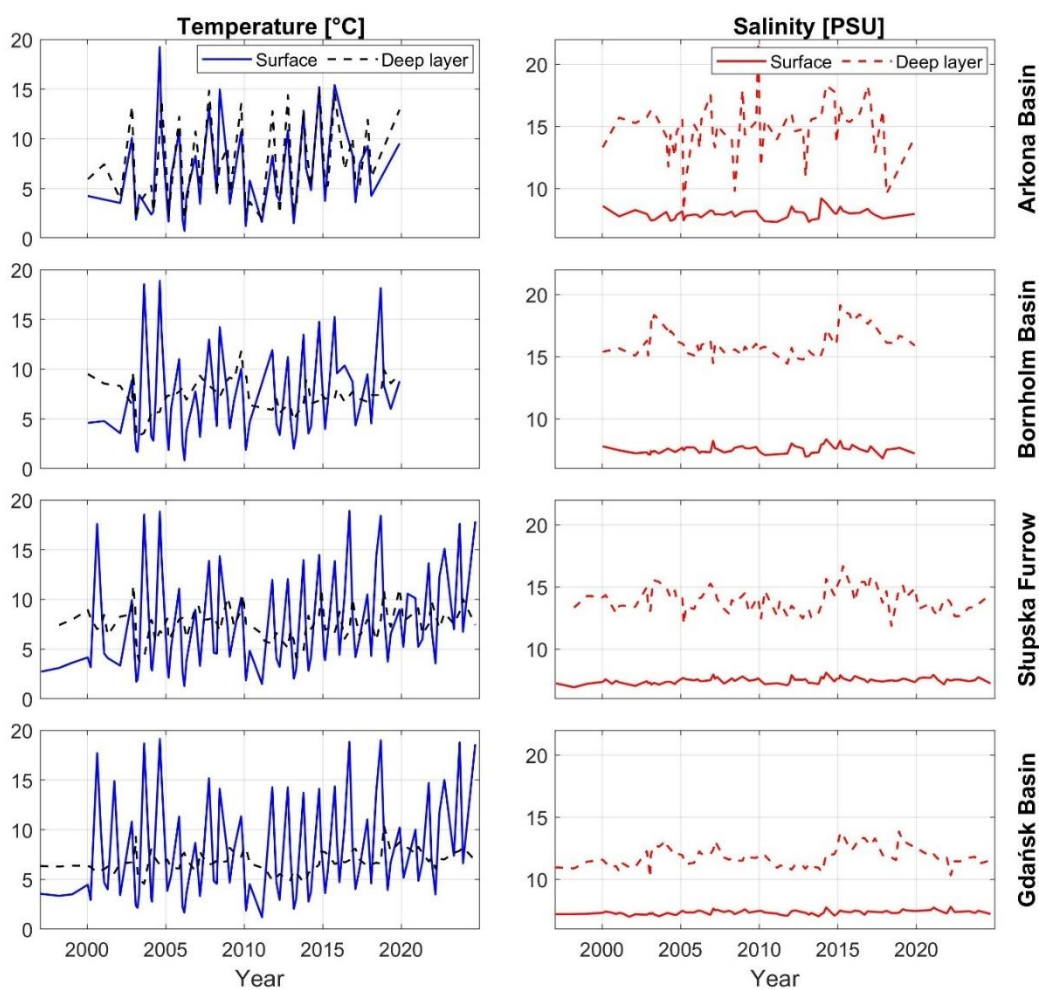


394

395 **Figure 9: Mean salinity (1997–2024) section along the repeat Baltic transect, shown as a function of longitude (°E) and**
 396 **pressure (dbar).**

397 Complementary basin-mean time series of layer-averaged temperature and salinity (Figure 10) illustrate how this
 398 vertical structure evolves in time. The 0–10 dbar surface layer is characterized by large interannual variability in
 399 temperature and relatively modest changes in salinity, reflecting the combined influence of atmospheric forcing,
 400 riverine input, and local mixing. In contrast, the bottom layer (defined consistently as the interval from 20 dbar
 401 above the seabed down to the bottom) varies more episodically, with pronounced salinity and temperature
 402 anomalies associated with inflow-driven ventilation events and subsequent stagnation periods. Along the transect,
 403 deep-layer signals are particularly pronounced in the Arkona Basin and in the deeper Bornholm Basin and Słupsk
 404 Furrow, and become progressively attenuated toward the Gdańsk Basin, in line with the downstream
 405 transformation of dense inflow waters inferred from the vertical structure in Figure 7. The comparatively strong
 406 deep-layer signals observed in the Arkona Basin reflect its position as the first basin reached by North Sea inflow
 407 waters entering the Baltic. These newly arrived waters retain high salinity and oxygen content and have undergone
 408 limited dilution or mixing, leading to pronounced anomalies. Farther east, in the Bornholm Basin and Słupsk
 409 Furrow, the same inflow waters are progressively modified through mixing and entrainment (Bulczak and Rak,
 410 2026), which reduces the amplitude of deep-layer signals.

411



412

413 **Figure 10: Basin-mean time series of layer-averaged temperature (left) and salinity (right) in the Arkona, Bornholm,**
 414 **Słupsk Furrow and Gdańsk basins for 1997–2024. Solid lines show the surface layer (0–10 dbar), while dashed lines**
 415 **show a bottom layer defined uniformly from 20 dbar above the bottom down to the bottom in each basin.**

8. Conclusion

We present a unique, quality-controlled CTD dataset spanning 1997–2024, assembled along a repeat section from the Arkona Basin through the Bornholm Basin and Słupsk Furrow to the Gdańsk Basin. In total, 96 cruises and 55,032 profiles were collected, providing rare temporal continuity and along-track resolution for the southern Baltic Sea.

The observing system evolved from high-rate towed profiling to a hybrid approach that, since 2020, also includes vertical station casts with a nominal ≤ 5 nm spacing. Instrumentation progressed from Guildline 87104 and Idronaut OS316 to Sea-Bird SBE49 and SBE19plus, and most recently Idronaut OS316Plus—choices driven by sampling-rate capability and robust telemetry. Together, these modes and sensors yield horizontal scales of ~200–500 m at ~4 kn in 60–120 m depths and enable both down- and up-cast sampling in tow.

A consistent processing chain—standardized parsing of CNV/TXT, robust time/position handling, binning to 1 dbar, median filtering, automated geolocation QC, and pruning of incomplete casts—ensures inter-comparability through time and across instruments. The final distribution package (IOPAN_Baltic.mat) provides cruise-wise fields (BMMYY) with 1-dbar vertical grids, co-registered P–T–S matrices, and MATLAB serial-day time stamps (UTC), ready for analysis and conversion.

We explicitly acknowledge limitations that inform interpretation: reduced summer coverage due to Arctic commitments; tow-induced horizontal uncertainty comparable to the local depth (with typical offsets $\approx 0.5 \times$ depth; see Section Instrument calibration and uncertainty budget); and a marked post-2020 decline in sampling linked to the loss of the SBE49 towed system (May 2020) and COVID-19 constraints. These variations predominantly reflect instrument availability, logistics, and weather rather than changes in QC or processing.

Despite these constraints, the dataset fills a long-standing observational gap in the Polish EEZ, where long, high-resolution CTD time series have been scarce, thereby strengthening model validation, reanalysis, and process studies of stratification, mixing, and inflow-driven ventilation along hydraulic controls. The section also serves as a reference line for quality control and validation of Baltic Argo float profiles and other autonomous observations, anchoring their measurements in a well-characterized hydrographic framework.

By making the full resource publicly available in both MATLAB and CF-compliant NetCDF formats, with transparent methods and structure, we provide an immediate foundation for multi-scale studies—from seasonal to decadal variability in temperature and salinity to the propagation and transformation of North Sea inflows—and for data assimilation in regional models. Continued observations along this established transect, ideally with renewed high-rate towed capability and routine auxiliary sensors (e.g., dissolved oxygen, turbidity) leveraging the OS316Plus pass-through interface, will be essential for tracking ongoing hydrographic change and supporting evidence-based management in the Baltic Sea.

450
451
452
453
454
455
456
457
458
459
460
461
462
463
464
465
466
467
468
469
470
471
472
473
474
475
476
477
478
479

Code availability

The MATLAB scripts used to build the processed IOPAN structure (Rak, 2025) from raw exports and to generate the CF-1.8 NetCDF products (build_IOPAN_from_CNV_TXT.m and write_IOPAN_to_netcdf.m) are archived on Zenodo at <https://doi.org/10.5281/zenodo.17814769>.

Data availability

The full dataset (Rak, 2025) is available from <https://doi.org/10.48457/IOPAN.2025.531> in two formats: a single MATLAB file (IOPAN_Baltic.mat) containing all cruises as the IOPAN struct, and a collection of per-cruise, CF-1.8-compliant NetCDF files (IOPAN_BMMYY.nc, one file per cruise). Both formats provide the same gridded hydrographic fields and associated metadata, enabling straightforward use in MATLAB, Python and other common analysis environments.

Author contribution

DR coordinated the compilation of the IOPAN CTD dataset, designed the processing and quality-control workflow, processed and quality-controlled the data, developed the MATLAB processing and NetCDF export scripts, and prepared the figures and the initial manuscript draft. All authors contributed to CTD data acquisition during the cruises, participated in discussions on data interpretation and quality assessment, reviewed the manuscript, and approved the final version.

Competing interests

The authors declare that they have no conflict of interest.

Acknowledgements

We gratefully acknowledge the late Prof. dr hab. Jan Piechura, co-author of this study, for his invaluable contribution to the collection of the hydrographic data used here. We also thank the crew of r/v Oceania for their long-term support during the field campaigns.

Funding

This publication was supported by the following project: Argo-Poland, funded by the Polish Minister of Education and Science [grant number 2022/WK/04].

480 **References**

481

482 Bulczak, A. I., Nowak, K., Jakacki, J., Muzyka, M., Rak, D., & Walczowski, W. (2024). Seasonal variability and
483 long-term winter shoaling of the upper mixed layer in the southern Baltic Sea. *Continental Shelf Research*, 276,
484 105232. <https://doi.org/10.1016/j.csr.2024.105232>

485 Bulczak A.I and Rak D (2026). Propagation and mixing of the 2023/24 inflow: impacts on stratification
486 and deep-water ventilation in the Southern Baltic Sea. *Front. Mar. Sci.* 13:1629491.
487 <https://doi.org/10.3389/fmars.2026.1629491>

488 Burchard, H., Lass, H.-U., Mohrholz, V., Umlauf, L., Sellschopp, J., Fiekas, V., Bolding, K., & Arneborg, L.
489 (2005). Dynamics of medium-intensity dense water plumes in the Arkona Basin, Western Baltic Sea. *Ocean*
490 *Dynamics*, 55(5), 391–402. <https://doi.org/10.1007/s10236-005-0025-2>

491 Feistel, R., Nausch, G., & Wasmund, N. (Eds.). (2008). *State and Evolution of the Baltic Sea, 1952–2005: A*
492 *detailed 50-year survey of meteorology and climate, physics, chemistry, biology, and marine environment*.
493 Wiley.

494 Fischer, H., & Matthäus, W. (1996). The importance of the Drogden Sill in the Sound for major Baltic inflows.
495 *Journal of Marine Systems*, 9(3–4), 137–157. [https://doi.org/10.1016/S0924-7963\(96\)00046-2](https://doi.org/10.1016/S0924-7963(96)00046-2)

496 Gröger, M., Dieterich, C., Haapala, J., Ho-Hagemann, H. T. M., Hagemann, S., Jakacki, J., May, W., Meier, H.
497 E. M., Miller, P. A., Rutgersson, A., and Wu, L. (2021). Coupled regional Earth system modeling in the Baltic
498 Sea region. *Earth System Dynamics*, 12, 939–973. <https://doi.org/10.5194/esd-12-939-2021>

499 Leppäranta, M., & Myrberg, K. (2009). *Physical Oceanography of the Baltic Sea*. Springer.
500 <https://doi.org/10.1007/978-3-540-79703-6>

501 Matthäus, W., & Franck, H. (1992). Characteristics of major Baltic inflows—A statistical analysis. *Continental*
502 *Shelf Research*, 12(12), 1375–1400. [https://doi.org/10.1016/0278-4343\(92\)90060-W](https://doi.org/10.1016/0278-4343(92)90060-W)

503 Mohrholz, V., Naumann, M., Nausch, G., Krüger, S., & Gräwe, U. (2015). Fresh oxygen for the Baltic Sea—An
504 exceptional saline inflow after a decade of stagnation. *Journal of Marine Systems*, 148, 152–166.
505 <https://doi.org/10.1016/j.jmarsys.2015.03.005>

506 Mohrholz, V. (2018). Major Baltic inflow statistics—Revised. *Frontiers in Marine Science*, 5, 384.
507 <https://doi.org/10.3389/fmars.2018.00384>

508 Omstedt, A., Elken, J., Lehmann, A., Leppäranta, M., Meier, H. E. M., Myrberg, K., & Rutgersson, A. (2014).
509 Progress in physical oceanography of the Baltic Sea during the 2003–2014 period. *Progress in Oceanography*,
510 128, 139–171. <https://doi.org/10.1016/j.pocean.2014.08.010>

511 Rak, D. (2016). The inflow in the Baltic Proper as recorded in January–February 2015. *Oceanologia*, 58(3), 241–
512 247. <https://doi.org/10.1016/j.oceano.2016.04.001>

513 Rak, D. (2025). IOPAN Baltic CTD processing and CF-1.8 NetCDF export (MATLAB) (1.0.0). Zenodo.
514 <https://doi.org/10.5281/zenodo.17814769>

515 Rak, D. (2025). Southern Baltic Sea hydrographic CTD profiles along the Arkona–Bornholm–Ślupsk–Gdańsk
516 transect (1997–2024). Geonetwork. <https://doi.org/10.48457/IOPAN.2025.531>

517 Rak, D., Przyborska, A., Bulczak, A. I., & Dzierzbicka-Głowacka, L. (2024). Energy fluxes and vertical heat
518 transfer in the Southern Baltic Sea. *Frontiers in Marine Science*, 11, 1365759.
519 <https://doi.org/10.3389/fmars.2024.1365759>

520 Rak, D., Walczowski, W., Dzierzbicka-Głowacka, L., & Shchuka, S. (2020). Dissolved oxygen variability in the
521 southern Baltic Sea in 2013–2018. *Oceanologia*, 62(4, Part A), 525–537.
522 <https://doi.org/10.1016/j.oceano.2020.08.005>

523 Rak, D., & Wieczorek, P. (2012). Variability of temperature and salinity over the last decade in selected regions
524 of the southern Baltic Sea. *Oceanologia*, 54(3), 339–354. <https://doi.org/10.5697/oc.54-3.339>

525 Reissmann, J. H., Burchard, H., Feistel, R., Hagen, E., Lass, H. U., Mohrholz, V., Nausch, G., Umlauf, L., &
526 Wieczorek, G. (2009). Vertical mixing in the Baltic Sea and consequences for eutrophication—A review.
527 *Progress in Oceanography*, 82(1), 47–80. <https://doi.org/10.1016/j.pocean.2007.10.004>

528 Stigebrandt, A., & Gustafsson, B. (2003). The response of the Baltic Sea to climate change – Theory and
529 observations. *Journal of Sea Research*, 49(4), 243–256. [https://doi.org/10.1016/S1385-1101\(03\)00021-2](https://doi.org/10.1016/S1385-1101(03)00021-2)

530 Walczowski, W., Merchel, M., Rak, D., Wieczorek, P., & Goszczko, I. (2020). Argo floats in the southern Baltic
531 Sea. *Oceanologia*, 62(4, Part A), 478–488. <https://doi.org/10.1016/j.oceano.2020.07.001>